Advanced Industrial and Engineering Polymer Research 2 (2019) 32–41

Contents lists available at ScienceDirect

Advanced Industrial and Engineering Polymer Research

journal homepage: http://www.keaipublishing.com/aiepr

Fundamental researches on graphene/rubber nanocomposites

Hao Zhang, Wang Xing, Hengyi Li, Zhengtian Xie, Guangsu Huang, Jinrong Wu*

State Key Laboratory of Polymer Materials Engineering, College of Polymer Science and Engineering, Sichuan University, Chengdu, 610065, China

ARTICLE INFO

Article history:
Received 2 November 2018
Received in revised form
9 January 2019
Accepted 11 January 2019

Keywords:
Graphene
Rubber
Nanocomposite

ABSTRACT

Graphene has exceptionally high surface area, mechanical properties, electrical conductivity, thermal conductivity, and gas-barrier performance, thus it is considered as an ideal multifunctional filler for rubbers. However, harnessing these properties in rubber nanocomposites requires us to carefully tailor the dispersion state of graphene, the vulcanization kinetics, the interfacial interaction and so on. This review summarized our recent works on how to disperse graphene homogeneously in rubber matrix, what influence of graphene or graphene oxide on the vulcanization behavior of the rubber nanocomposites, how to design a compact filler network in the rubber matrix, and how to engineer a strong interfacial interaction between graphene and rubber. These fundamental researches give us some thumb rules to develop graphene/rubber nanocomposites with significantly improved mechanical properties, gas-barrier performance, thermal stability, electric conductivity, antioxidation ability as well as some functionalities.

© 2019 Kingfa SCI. & TECH. CO., LTD. Production and Hosting by Elsevier B.V. on behalf of KeAi Communications Co., Ltd. This is an open access article under the CC BY-NC-ND license (http://creativecommons.org/licenses/by-nc-nd/4.0/).

1. Introduction

Rubbers are widely used in many fields, such as vehicle engineering, aerospace exploration, biomedical applications, civil applications and so on. However, unfilled rubbers usually show poor mechanical properties. Thus, it is necessary to reinforce the rubbers with various fillers, such as carbon black, silica and clay. With these fillers, one can easily tune the modulus, tensile strength, elongation at break and toughness of rubbers for different applications. Nevertheless, the rapid development of advanced technologies requires rubber products with even higher mechanical performances as well as some advanced functions [1]. As such, it is highly desirable to search for novel nanomaterials, which cannot only reinforce rubbers but also confer them with new functions [1–3].

In the last decade, graphene (GE) has attracted tremendous attention in the fields of materials and physics since it was firstly discovered by Geim and his coworkers in 2004 [4,5]. Graphene has a one-atom-thick planar structure composed of sp^2 hybridized carbon atoms packed in a honeycomb-like lattice. Due to this unique structure, graphene has extraordinarily high mechanical performance, electronic mobility, thermal conductivity and gas impermeability [6–8]. If these properties can be harnessed in rubbers, the resulting rubber nanocomposites will show greatly improved mechanical properties as well as some functionalities. As such, graphene is considered as an ideal multifunctional nanofiller for rubbers.

Yet, fabricating rubber/graphene nanocomposites needs to address several issues, such as how to homogeneously disperse graphene in rubber matrix, what influence of graphene or graphene oxide on the vulcanization behavior of the rubber nanocomposites, how to design a compact filler network in the rubber matrix, and how to engineer a strong interfacial interaction between graphene and rubber. Regarding these issues, a lot of efforts have been made in the area of rubber/graphene nanocomposites. Several works explored the influence of different compounding methods on the dispersion state of graphene [9–12]. It is found that with the improved dispersion, the rubber/graphene nanocomposites could achieve higher mechanical performance than traditional rubber-based composites [13–15]. Some works used surface functionalization to tailor the interfacial interaction between graphene and rubber matrices [16–22]. A strong interfacial interaction is proven to be critical to realize the reinforcement effect of graphene. Moreover, graphene is also utilized to improve the gas barrier performance, electrical conductivity and thermal conductivity of rubber nanocomposites [23–26]. Such a combination of different properties and functionalities of rubber/graphene nanocomposites has not only raised increasing interest in scientific community, but also opened new avenues for rubber industry.

* Corresponding author.
E-mail address: wujinrong@scu.edu.cn (J. Wu).

https://doi.org/10.1016/j.aiepr.2019.01.001
2542-5048/© 2019 Kingfa SCI. & TECH. CO., LTD. Production and Hosting by Elsevier B.V. on behalf of KeAi Communications Co., Ltd. This is an open access article under the CC BY-NC-ND license (http://creativecommons.org/licenses/by-nc-nd/4.0/).

In recent years, our group has been making continuous efforts toward exploring the fundamentals of rubber/graphene nanocomposites. We developed an efficient latex mixing approach to disperse graphene well in rubber and studied the vulcanizing mechanism of the graphene in rubber. We also studied the interface interaction and mechanical properties of the nanocomposite. Besides, we fabricated a series of novel rubber products and broadened the application of the graphene/rubber nanocomposites. In this review, we summarize our related works on the graphene/rubber nanocomposites, and provide some fundamental understanding toward these materials.

2. Preparation of graphene/rubber composites

2.1. Latex mixing

Since graphene is considered as an ideal multifunctional filler for polymers, several methods have been developed to incorporate graphene into polymer matrices, including solution mixing, in-situ polymerization, melt blending and latex mixing [1–3]. Although it's effective to obtain well-dispersed graphene nanosheets throughout the polymer matrix via in-situ polymerization and solution mixing [24], there are still some limitations such as the waste and probable pollution of the solvent, and the negative effect of graphene on the polymerization process. With the high production efficiency, melt blending is the most economical method to obtain bulk materials. Unluckily, the self-aggregation of graphene nanosheets caused by strong van der Waals force seems to be unpreventable which could be a great obstacle for its practical application [27].

Recently, latex compounding technology has been successfully developed to overcome these difficulties; it enables good dispersion of graphene sheets in polymer matrices without extra solvents. Actually, the latex compounding technology can be subdivided into two categories: in situ emulsion polymerization and latex mixing. Since most rubber products are produced in the form of latex, the latter category has become a more practical choice. However, there are still some problems to obtain a stable aqueous dispersion of graphene. It seems to be a possible approach to chemically reduce graphene oxide (GO) in the presence of the surfactant [11,28]. Nevertheless, the presence of foreign stabilizers is undesirable for the mechanical and electrical properties of the nanocomposites [29,30]. With the aid of sonication, researchers can disperse GO in the polymer latex and then reduce GO to graphene [31]. However, this approach will unfortunately lead to degradation of polymers and a great demand of energy.

Our group [32–34] has developed a facile approach based on latex blending without using additional stabilizer or sonication. In this approach (Fig. 1), an aqueous dispersion of GO was firstly mixed with polymer latex, then the mixture was co-coagulated with demulsifiers to form a suspension of particles in which GO nanosheets were isolated by polymer matrices. Finally, hydrazine hydrate was added to reduce GO in situ. With this well-modified approach, we obtained graphene/polystyrene nanocomposites with both high electrical conductivity and improved mechanical properties [35]. The electrical conductivity of a composite with a load of 8.0 wt% of graphene is 11 orders of magnitude higher than that of pure polystyrene, as a result of the formation of conductive network in the polymer matrix. The dynamic mechanical properties such as storage modulus of the nanocomposites are greatly improved by the incorporation of graphene. Moreover, we successfully applied this method to the fabrication of the graphene/rubber nanocomposites with excellent mechanical performances and other functions which would be discussed later.

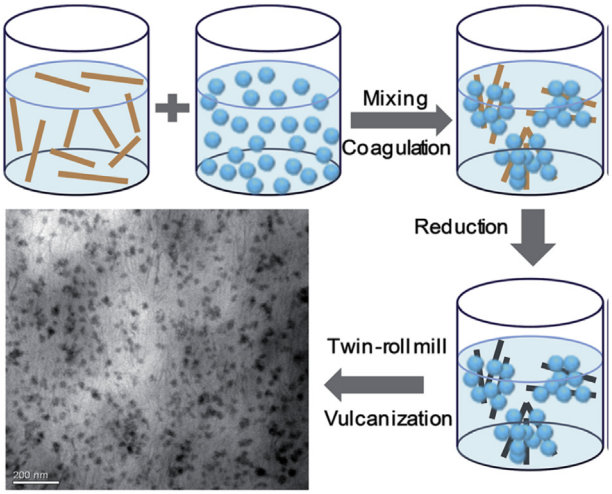


Fig. 1. Preparation and morphology of the styrene butadiene rubber (SBR)/GE nanocomposites. Schematic description of the modified latex compounding method, and the transmission electron microscope (TEM) image of the nanocomposites which demonstrates the homogeneous dispersion of graphene nanosheets [34].

2.2. Vulcanization

It is well-known that the vulcanization state plays a key role in the mechanical properties of rubbers. There have been many investigations on the vulcanization reactions and kinetics of unfilled rubbers [36]. Some recent studies have shown that the vulcanization kinetics of rubbers could be changed significantly by incorporation of nanofillers. Researchers have studied the influence of organoclay and carbon nanotubes [37–41]. Others have also worked on the functional group of the nanofillers and studied the influences of the different groups on the vulcanization [42,43]. However, the influence of graphene on the vulcanization kinetics of rubbers, which is one of the most critical issues in the preparation of graphene/rubber nanocomposites, has not been well studied. Few works reported the accelerating effect of graphene, while the details of the vulcanization kinetics and the underlying mechanism have not been well investigated [23,44].

Our group [45] systematically studied the vulcanization kinetics of the graphene/natural rubber (GE/NR) nanocomposites prepared by the modified latex mixing method (Fig. 2). Curemeter and differential scanning calorimetry (DSC) measurements were carried out and the results indicated that the addition of a small amount of graphene greatly changed the vulcanization kinetics of NR. The induction period of the vulcanization process was drastically suppressed at low graphene loading and then showed a gentle decrease, while the vulcanization rate was enhanced firstly and subsequently showed a depression. The combination effect of these two aspects led to a prominent reduction in optimum cure time at first and then a slight increase. Unfilled NR and GE/NR nanocomposites with graphene loading less than 0.3 phr displayed a single exothermal peak during the vulcanization process, while that with higher loading was split into two peaks at higher graphene loading. We proposed that the physical diffusion process of the curing agents might be the reason. Thus, the two peaks were the results of two reaction stages, the chemical reaction controlling stage and the diffusion controlling stage. The chemical reaction controlling stage had lower activation energy than the latter stage. Addition of graphene decreases the activation energy of the former stage, and it had an opposite effect on the activation energy of the latter stage. Finally, we proposed a possible mechanism to interpret the accelerating effect of graphene on NR. The current work

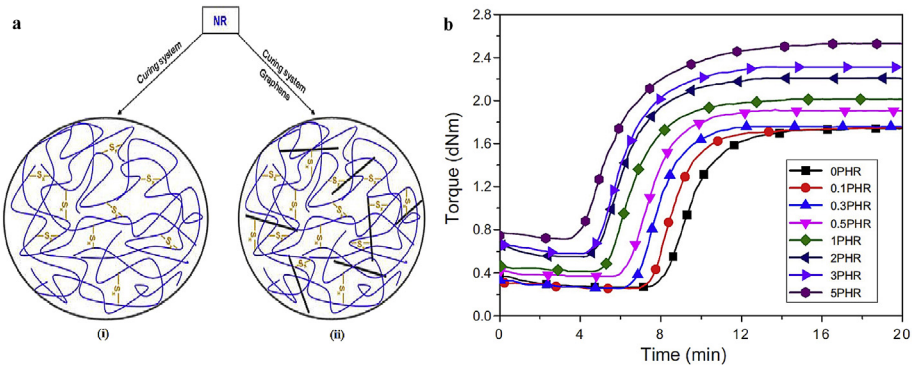


Fig. 2. (a) Schematic representation of the network structures of unfilled NR (i) and GE/NR nanocomposites (ii); (b) curing curves of NR and GE/NR nanocomposites with different graphene loadings [45].

indicated that graphene could be used to tune the vulcanization kinetics of rubbers, in addition to the mechanical properties, gas permeability and electrical conductivity.

The fabrication of rubber products requires the addition of both fillers and curing agent, which is very tedious and energy consuming due to the long time of mechanical mixing to ensure homogenous dispersion of curing agents and fillers in the matrix. In addition, the chemical activity of curing agents and the amounts of the activator and the accelerator that regulate the crosslinking rate must be carefully balanced. To simplify this process, it is highly desirable to develop a method that enables crosslinking and reinforcement of rubbers through a one-step process.

It seems to be a possible strategy to develop particles that have dual functions in order to circumvent the difficulties during rubber processing. In this way, particles should not only act as fillers, but also be able to crosslink rubbers. Unfortunately, both the traditional fillers such as carbon black and modern nanofillers such as graphene cannot serve as crosslinking agents [21,36,45]. In a previous work, we developed a method to simultaneously crosslink and reinforce rubbers using graphene oxide [46]. Upon heating, the chemically unstable oxygen-containing groups on graphene oxide undergo homolytic cleavage, which generates diffusive free radicals on oxygen-containing groups and localized free radicals on graphene oxide. The diffusive free radicals leads to chemical crosslinks in the rubber matrix, while the localized free radicals results in interfacial crosslinks between GO nanosheets and rubber matrix. Apparently, the crosslinking density on the interfaces is much higher than that in the matrix. Moreover, the physical CH-π interactions could absorb polymers onto the GO surface. The chemical crosslinks and physical interactions on the interfaces create theGO surface coated with polymers forming a carpet-like structure, thereby significantly increases the interfacial interaction between GO and rubber matrix.

As a result of the curing process caused by GO, the mechanical properties (such as the storage modulus and tensile strength) of GO/SBR nanocomposites are higher than those of SBR crosslinked by conventional method, and the properties can be further improved by tuning the fraction of GO. Importantly, the existence of an interfacial layer between polymers and GO surface adds an additional dimension to the parameter space for tuning the properties of GO/SBR nanocomposites. Usually, quantitative understanding of the thickness for interfacial layer and its role in affecting the mechanical properties of the nanocomposites is difficult. Our system provides a model system to explore the effects of interfacial layer on the mechanical properties of GO/rubber nanocomposites. By measuring the viscoelastic properties by dynamic mechanical analysis, we were able to estimate the thickness of the interfacial layer to about 10 nm. Therefore, due to the strong interfacial interaction and crosslinking reaction, graphene oxide not only reinforces the rubber by acting as fillers, but also is able to generate radicals that induce chemical crosslinking of the rubber (Fig. 3).

3. Properties and applications

3.1. Interface interaction

To improve the interfacial interaction of GE with rubber matrix, the surface modification of GE could be regarded as one of the most versatile strategies. But it is not practical to obtain a large amount of functionalized GE by direct modification of the defect-free GE. The current state is still based on the modification and reduction of graphene oxide. Moreover, the dispersion state also largely relies on the interfacial interaction. Various chemical reagents such as amino acids [47], polyvinyl alcohol [48] and orthoquinone-thiol chemistry [21] have been used to modify GO. These surface modifications eventually lead to enhanced interfacial interaction. However, it is still a challenge to acquire a conclusive relationship between the enhanced interfacial interaction and the macroscopic performance, which is an important issue to understand the reinforcing mechanism of nanoparticles.

In our research [23], GO is chemically modified with bis(triethoxysilylpropyl)tetrasulfide (BTESPT) through a facile process. The resulting surface functionalized graphene oxide (SGO) can be finely dispersed in NR at low filler loading and has strong interfacial interaction with the NR matrix. Therefore, the mechanical performance and the gas barrier property of NR are significantly improved at very low content of fillers. With only 0.3 wt% of SGO, a 100% increase in the tensile strength, a 66% improvement in the tensile modulus and a 48% reduction in the air permeability of NR are achieved. The results reveal that surface functionalized graphene oxide has wide applications in improving the mechanical and gas barrier properties of rubber-based nanocomposites.

Furthermore, SGO was employed to prepare isoprene rubber/surface modified GE (IR/SGE) composites by solution blending and in-situ reduction [49]. The height profile obtained from atomic force microscope (AFM) shows that the thickness of a single-layer GO sheet is about 1 nm, while a single-layer SGO sheet has a thickness of about 1.5 nm. The increase in thickness confirms that the BTESPT molecules are successfully grafted onto the surfaces of SGO. The functionalized SGO can be well dispersed and reduced into SGE in rubber matrix (Fig. 4). By using Raman mapping, the morphology of bound rubber on SGE and GE was observed. The mapping images show that there is a thick layer of IR molecules adsorbed on the surface of SGE, while little rubber can be detected on the surface of GE. Since the samples were fully extracted with toluene, the residual bound rubber could be attributed to the strong

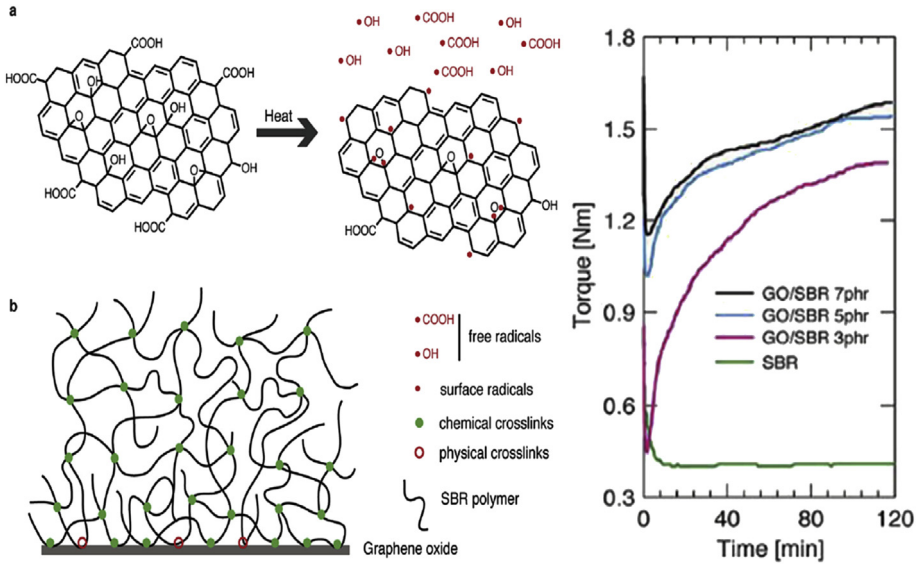


Fig. 3. A schematic description of the crosslinking mechanism of GO and the curing curves of pure SBR and GO/SBR nanocomposites at 170 °C. The homolytic cleavage of oxygenic groups on GO produces two categories of free radicals, including free radicals on cleaved groups and free radicals on GO. The free radicals on the cleaved group can diffuse away from GO and lead to crosslinking of the rubber matrix; while the free radicals on GO are localized and result in interfacial crosslinking between GO and SBR. In addition to chemical crosslinks induced by free radicals, there are also physical crosslinks (empty circles) due to the absorption of polymers onto GO. The crosslinking density decreases as the distance from the GO surface increases, and eventually becomes a constant [46].

interfacial interaction between the filler particle and rubber matrix. From the perspective of molecular dynamics, broadband dielectric spectroscopy reveals that the addition of SGE results in a stronger confinement to IR molecular chains than that of GE.

The confinement effect of nanofillers not only affects the molecular dynamics but also changes the strain induced crystallization (SIC) behavior of rubber nanocomposites. To explore this effect, we used in situ synchrotron wide-angle X-ray diffraction (WAXD) experiments to measure the SIC of IR/SGE, and the results were compared with that of unfilled IR and IR/GE nanocomposites (Fig. 5). It can be found that the oriented arc of IR/SGE appears much earlier than that of unfilled IR, indicating that the incorporation of SGE facilitates SIC of IR. This phenomenon can be attributed to the strong interaction between nanofillers and rubber molecules. However, since the surface modification endows IR/SGE with stronger interfacial interaction and lower chain mobility, IR/SGE exhibits a lower crystallization rate than IR/GE.

Interestingly, on-line Raman measurement during the stretching process of IR/SGE and IR/GE nanocomposites suggests that the stronger interfacial interaction leads to more efficient load transfer in material. Thus, IR/SGE nanocomposites show superior mechanical properties than IR/GE nanocompositess.

3.2. Mechanical reinforcement

Most applications of rubbers cannot be envisaged without reinforcement, as crosslinked rubbers generally have low tensile strength and elongation. Typically, diene rubbers are reinforced

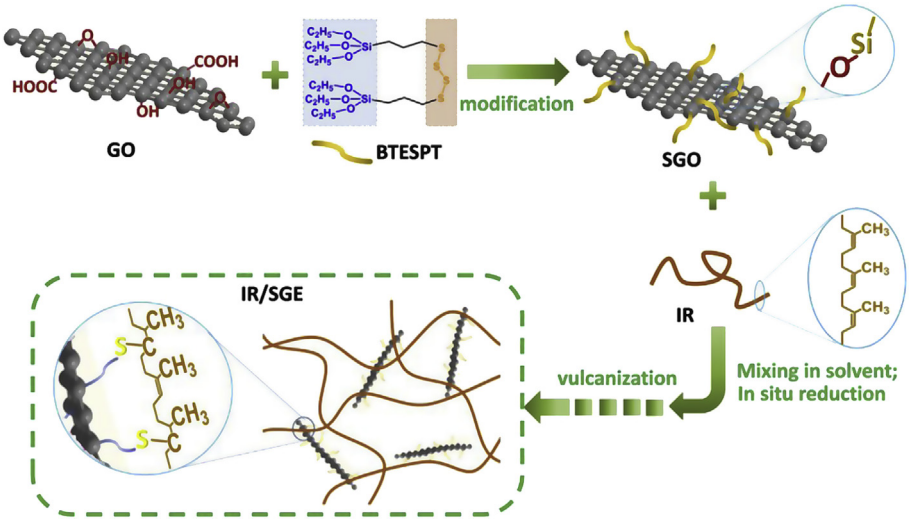


Fig. 4. Schematic diagram of the modification of GO and preparation of IR/SGE composites [49].

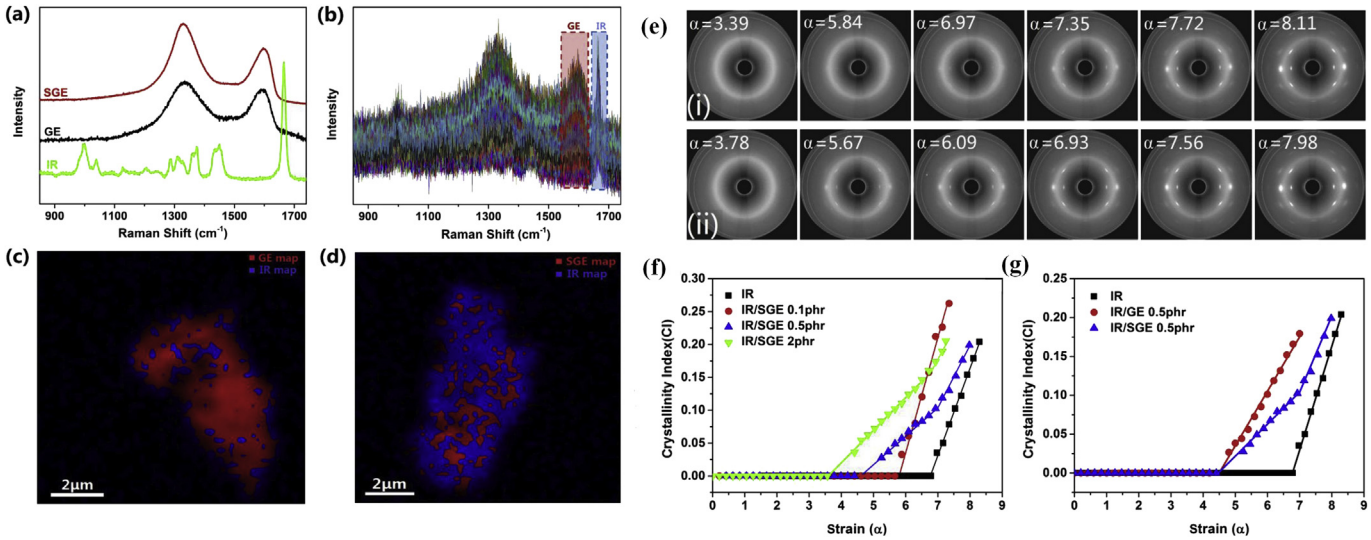


Fig. 5. (a) Raman spectrums of neat IR, GE and SGE sheet; (b) Raman mapping spectrums: red and blue region are integral region for GE mapping and rubber mapping, respectively; (c) Raman mapping image of GE with adsorption rubber; (d) Raman mapping image of SGE with adsorption rubber; (e) WAXD patterns of unfilled IR (i) and IR/SGE (ii) in various strains; (f) crystallinity index of IR/SGE with various filler contents as a function of strains; (g) crystallinity index of unfilled IR, IR/SGE and IR/GE with 0.5 phr filler as a function of strains [49].

with fillers, such as carbon black and silica. These fillers can form a filler network through agglomerates which can undergo reversible breakdown and reagglomeration upon deformation with energy dissipation [50–52]. However, to form a percolated filler network, the loading of carbon black and silica usually exceeds 30 phr, which greatly decreases the elongation due to the strain amplification effect and stress concentration at the agglomerates. Recently, it has been found that nanofillers, especially hybridizing GE with carbon nanotubes (CNTs), are more efficient for forming the filler networks. And it has been demonstrated that the compact filler network enables the GE/CNT hybrid to have synergistic effects in improving the mechanical strength, electrical conductivity and thermal stability of polymer nanocomposites [53–59]. Yet, the potential energy dissipation ability of the hybrid filler network and its toughening effects on rubbers remains to be explored.

Our group [60] developed a modified latex mixing method to homogeneously disperse the GE/CNT hybrid in natural rubber. We demonstrated that the GE/CNT hybrid could form a more compact filler network than single-component GE or CNTs. The physical interactions of the filler network can break and reform, and thus serve as sacrificial bonds and dissipate energy under cyclic loadings (Fig. 6). The larger energy dissipation capacity of the hybrid filler network not only leads to higher toughness and tensile strength (Fig. 7), but also results in a lower crack growth rate of the NR/GE/CNT nanocomposites. The GE/CNT hybrid outperforms most traditional fillers and single-component nanofillers in improving mechanical properties of NR. Considering the low filler loading of the GE/CNT hybrid compared with that of carbon black, silica and clay, such high toughening and reinforcement efficiencies are remarkable.

3.3. Anti-aging property

Due to the instability of unsaturated double bonds and active allylic hydrogens, diolefin elastomers such as natural rubber (NR) and styrene butadiene rubber (SBR) easily undergo thermal

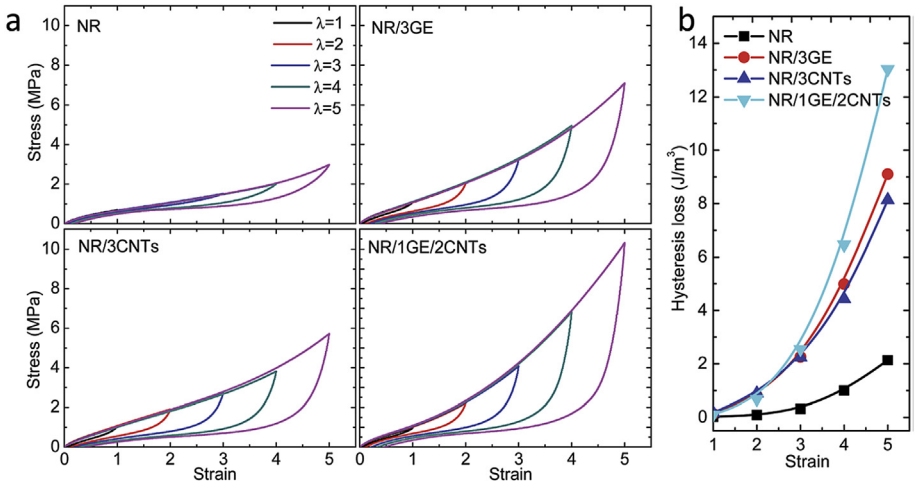


Fig. 6. Energy dissipation during the first tensile cycle. (a) Cyclic stress–strain curves and (b) hysteresis loss of the first tensile cycle of NR, NR/3GE, NR/3CNTs and NR/1GE/2CNTs [60].

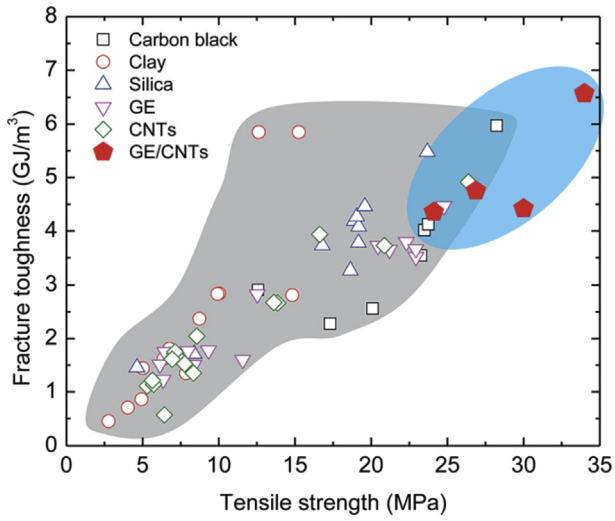


Fig. 7. Ashby plot in terms of fracture toughness versus tensile strength. The fillers for NR include carbon black, silica, clay, GE and CNTs [60].

oxidation, which results in scission of polymer chains and formation of extra crosslinks and oxygenic groups [61,62]. The aging process would be accompanied by the dramatic reduction of the mechanical properties, thus leading to decreased reliability and earlier failure of the rubber products. To deal with the problem, it is common to use the antioxidants to capture free radicals generated by oxidation. However, many additives are volatile with the low anti-aging efficiency, while some kinds of chemical methods to increase the anti-aging performance might not be scaled up to the industrial level due to their complex process. Nanofillers such as fullerene and carbon nanotubes could scavenge free-radicals from thermal oxidation through high electron affinity while layer-like nanofillers such as nanoclays could form barriers to prevent both the inward-diffusion of oxygen and the outward-diffusion of volatile decomposed products [63–67]. As a one-atom-thick two-dimensional nanosheet composed of sp^2 hybridized carbon, graphene is capable of both scavenging free-radicals and serving as gas barriers [10,23,24,68–70], which would enable graphene to be more effective in improving the thermal stability of elastomer/graphene nanocomposites.

Our group [34] reported that graphene would be a promising antioxidant to prevent the thermal oxidation and prolong the lifetime of SBR and systematically studied the long-term thermal oxidation process of the nanocomposites (Fig. 8). We homogeneously disperse graphene in SBR by a modified latex mixing method. We found that the diffusion pathways of small molecules are increased as a result of the homogeneous dispersion and the high aspect ratio of graphene. Besides, the cross-sections for gas diffusion are reduced, which strongly suppresses the oxygen permeability of the SBR/GE nanocomposites. Therefore, the oxygen permeability of the nanocomposites decreases with graphene loading. Moreover, electron paramagnetic resonance (EPR) measurements demonstrate that the SBR/GE nanocomposites have a much lower concentration of free radicals than the unfilled SBR, suggesting that the reduced graphene could absorb free radicals. Therefore, both the free-radical scavenging and gas barrier abilities of graphene contribute to the prolonged lifetime of the SBR/GE nanocomposites.

Moreover, we quantified the mechanical properties and chemical compositions of these nanocomposites during an accelerated ageing process, the results were compared with unfilled SBR.

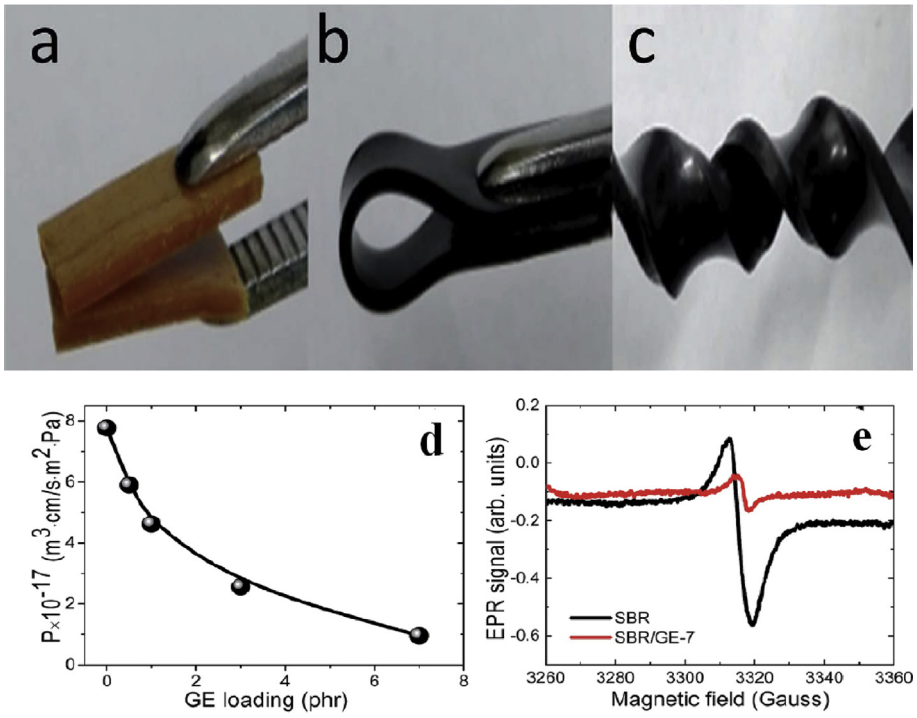


Fig. 8. The anti-aging property of the SBR composites. (a) The unfilled SBR ruptures after bending after thermal oxidative aging at 90 °C for 13 days; (b) and (c) the SBR/GE-7 is still flexible and remains intact when subjected to bending and twisting; (d) influence of graphene loading on the oxygen permeability of the SBR/GE nanocomposites; (e) first derivative of EPR spectra of the unfilled SBR and SBR/GE-7 after the thermal oxidative aging [34].

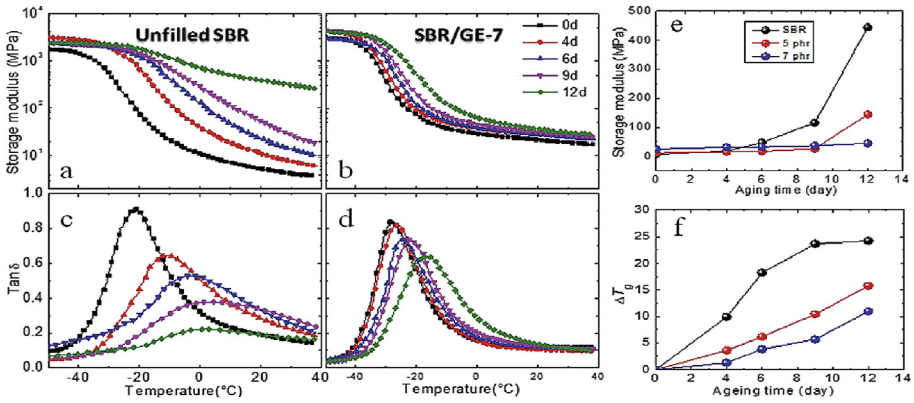


Fig. 9. Changes in the dynamic mechanical properties upon thermal oxidative aging: storage modulus (E′) vs. temperature curves of (a) the unfilled SBR and (b) the SBR/GE-7 on different ageing days; loss factor *vs.* temperature curves of (c) the unfilled SBR and (d) the SBR/GE-7 on different ageing days. Effect of ageing time on (e) the storage modulus at 10 °C, and (f) the T_g shift of the unfilled SBR and the SBR/GE nanocomposites with 5 phr and 7 phr of graphene [34].

The SBR/GE nanocomposites show a lower increase in the stiffness and T_g with a higher retention ratio of tensile strain and strength. Also, the O/C ratio in the SBR/GE nanocomposites is lower. The results suggest that the oxidation process of the SBR/GE nanocomposites is significantly delayed compared to the unfilled SBR. Therefore, the nanocomposites show less deterioration in chemical and mechanical properties and thus a longer lifetime during the aging process (Fig. 9).

3.4. Heat insulation

In the last years, much attention has paid to graphene based aerogels with special functions. For example, the thermal conductivity could be decreased to 15 mW m^{-1} K^{-1} by freeze-casting a suspension of graphene oxide, cellulose nanofibers and sepiolite nanorods [71]. Unfortunately, these kinds of aerogels do not show any shape-memory property, which inhibits the application in the irregular and small area.

We fabricated a novel hybrid aerogel with multiple networks to obtain both the low thermal conductivity and shape-memory property [72] (Fig. 10). We prepared a physical network of GO aerogel (first network), and then infuse the network with a solution of triblock copolymer, polystyrene-b-poly (ethylene-butylene)-b-polystyrene-g-maleic anhydride (SEBS). The functional groups on the triblock copolymer can react with GO, forming a GO crosslinked triblock copolymer network (second network). After removing the solvent, the triblock copolymer itself forms a physical network through phase separation between the hard and soft blocks (third

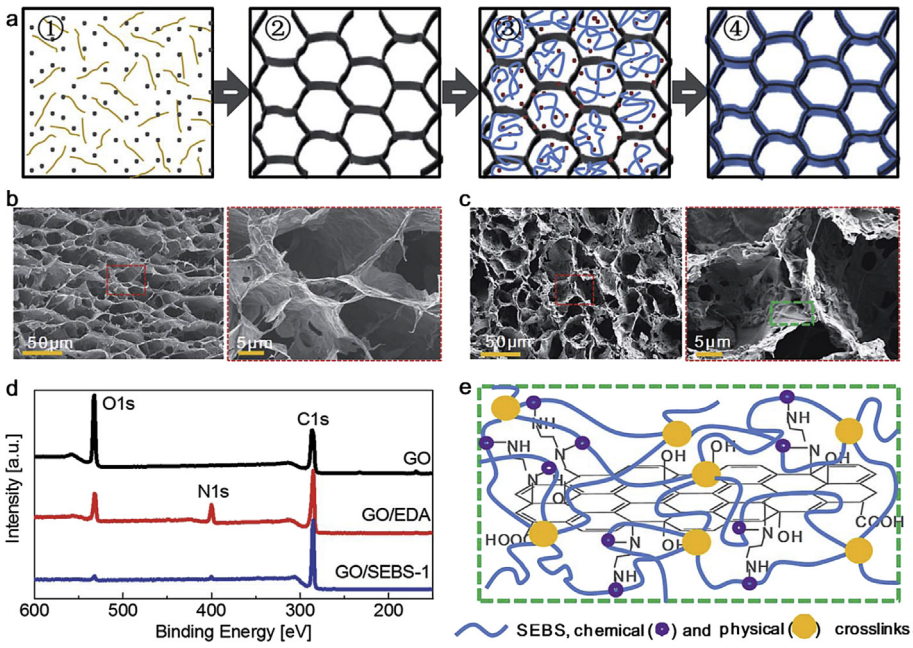


Fig. 10. Fabrication and microstructures of the aerogels. (a) Schematic description of the fabrication process of the hybrid aerogel. An aqueous suspension of GO (①) undergoes gelation with ethylenediamine and the gel is then freeze dried to form a GO aerogel (②). The GO aerogel is infused with a para-xylene solution of SEBS (③) and is further lyophilized to form a GO/SEBS hybrid aerogel (④). (b) scanning electron microscope (SEM) images of the GO aerogel. (c) SEM images of the GO/SEBS hybrid aerogel. (d) X-ray photoelectron spectroscopy (XPS) spectra of pristine GO nanosheets, GO aerogel and GO/SEBS-1. (e) Schematic description of the microstructure of the hybrid aerogels [72].

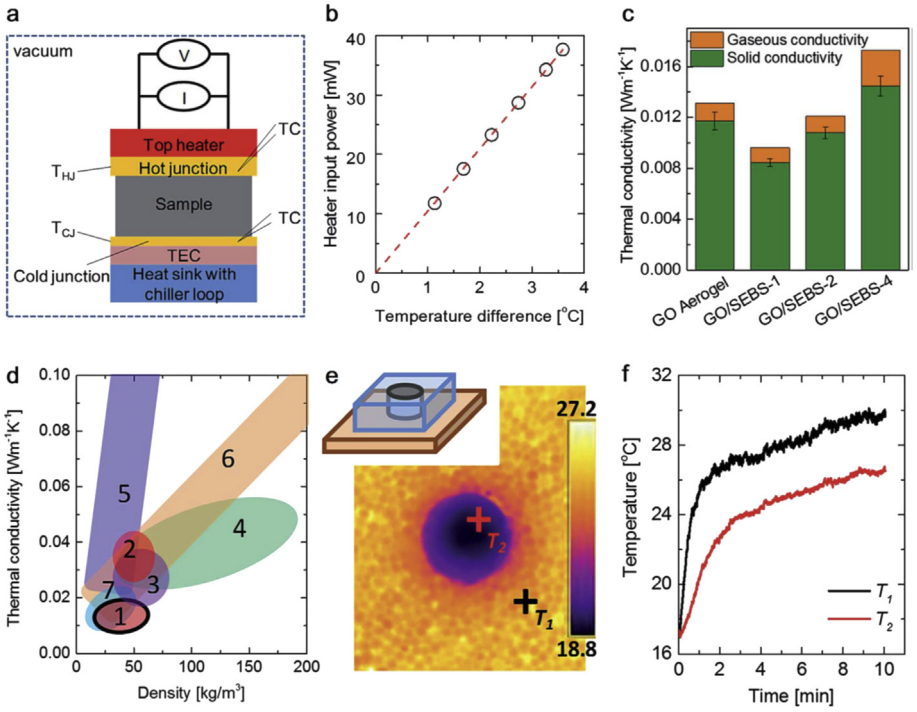


Fig. 11. Thermal conductivity of the aerogels. (a) Measurement of thermal conductivity of the aerogels using an in-house cooler-bridge steady state platform developed in the NanoEngineering Group of the Massachusetts Institute of Technology. (b) The measured heater input power as a function of temperature difference across the heating and cooling ends of an aerogel sample. The dashed line is a linear regression fit to the data. (c) Tested solid thermal conductivity and calculated gaseous thermal conductivity for GO and GO/SEBS aerogels. (d) A comparison of the thermal conductivity and apparent density of the GO/SEBS aerogels with those of other porous materials: (1) GO/SEBS hybrid aerogels; (2) expanded polystyrene; (3) polyurethane foam; (4) mineral wool; (5) carbon based aerogels; (6) silica aerogels; (7) phenolic resin aerogels. (e) Thermal image of a GO/SEBS-2 aerogel (gray) inserted in a sheet of expanded polystyrene foam (EPF, light blue). Measurement was done by placing the EPF on a heating plate of 48 °C (light brown) under an ambient temperature of 17 °C. The image was a snap-shot at 42 s. (f) Measured temperatures of the two points in (e) as a function of time. The black point is located on polystyrene foam, while the red point is located on the GO/SEBS-2 aerogel [72].

network). We found that the first network could serve as sacrificial bonds and dissipate energy upon deformation, resulting in the high mechanical performance of the aerogels. The second network allows the aerogels to memorize the original permanent shape due to its elastic nature, and third network is able to store strain energy and fix the aerogels in a temporary shape by vitrification. Most importantly, the interfaces between the three networks serve as phonon scattering centers that lead to an ultra-low thermal conductivity of the aerogels (Fig. 11). These mechanically strong and shape-memory aerogels with ultra-low thermal conductivity have great potential in a wide variety of thermal-insulating applications by improving the energy efficiency.

3.5. Other properties

To meet the new application demands of rubber materials, it is necessary to explore other properties of rubber/graphene nanocomposites. Upon achieving molecular level dispersion of GE nanosheets and strong interfacial interaction [73,74], we demonstrated that rubber/graphene nanocomposites have low heat buildup, improved wear resistance and thermal stability, remarkable gas impermeability and electricity conductivity (Figs. 12 and 13). Such versatile properties make the rubber/graphene nanocomposites a promising new class of advanced materials, which can be used in green tires and electronic skin.

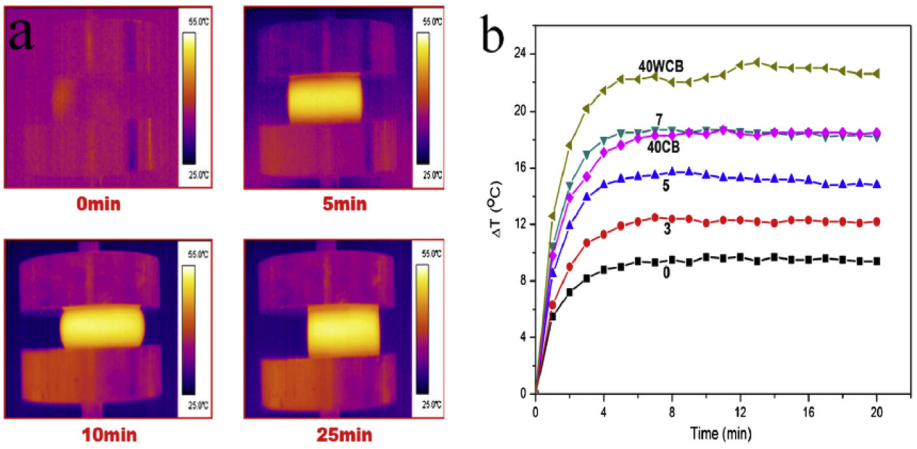


Fig. 12. (a) Images taken by infrared photography at different times and (b) heat buildup at ambient temperature (30 °C) as a function of compression time [74].

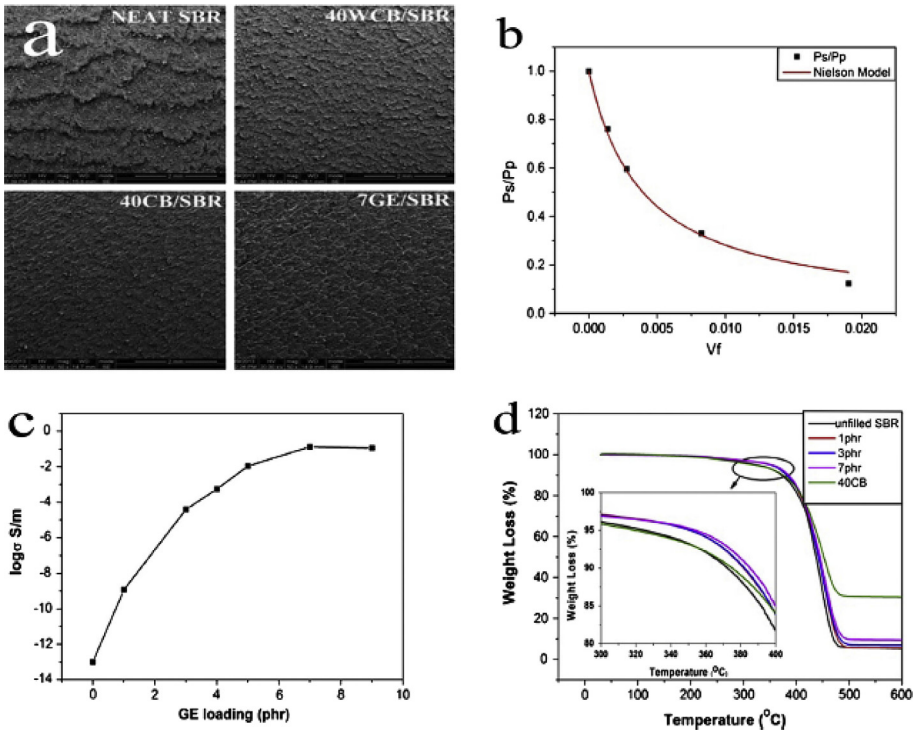


Fig. 13. (a) SEM images of abraded surfaces of unfilled SBR vulcanizate, 40 carbon black (CB)/SBR vulcanizate, 40 white carbon black (WCB)/SBR vulcanizate and 7GE/SBR nanocomposite; (b) oxygen permeability of GE/SBR nanocomposites normalized by that of unfilled SBR. The red solid line represents the prediction of the Nielson model; (c) electrical conductivity of GE/SBR nanocomposites as a function of GE loading; (d) thermogravimetric analysis (TGA) thermograms of unfilled SBR, 40WCB/SBR, 40CB/SBR and SBR nanocomposites with different GE loadings [74].

4. Conclusion

Our group has developed a modified method of the latex mixing to homogeneously disperse the graphene into the rubber matrix. During the vulcanization, we found that the graphene perform as the accelerating agent while graphene oxide has the function of curing agent. With the capability of both scavenging free-radicals and gas barriers, graphene can be utilized as an effective anti-aging agent in rubber products. Moreover, the hybrid network of the graphene and the carbon nanotubes could serve as sacrificial bonds and dissipate energy, which would dramatically improve the toughness of the rubber. Besides, with the novel design, graphene/rubber nanocomposites can be endowed with some special functions such as super heat insulation and shape memory, which greatly broaden the application area of the rubber products.

Conflict of interest

We declare that we have no conflicts of interest to this work.

Acknowledgements

This work was financially supported by the National Natural Science Foundation of China (grant No. 51673120) and Sichuan University.

References

[1] Zheng-Hai Tang, Bao-Chun Guo, Li-Qun Zhang, De-Min Jia, Acta Polym. Sin. (7) (2014) 865–877.
[2] Qiang Bu, Fang-Fang He, He-Sheng Xia, Acta Polym. Sin. (6) (2014) 715–723.
[3] X. Liu, L. Wang, L. Zhao, H. He, X. Shao, G. Fang, Z. Wan, R. Zeng, Polym. Compos. 39 (4) (2018) 1006–1022.
[4] K.S. Novoselov, A.K. Geim, S.V. Morozov, D. Jiang, Y. Zhang, S.V. Dubonos, I.V. Grigorieva, A.A. Firsov, Science 306 (5696) (2004) 666–669.
[5] T.O. Wehling, K.S. Novoselov, S.V. Morozov, E.E. Vdovin, M.I. Katsnelson, A.K. Geim, A.I. Lichtenstein, Nano Lett. 8 (1) (2008) 173–177.
[6] A. Barker, X. Du, I. Skachko, E.Y. Andrei, Nat. Nanotechnol. 3 (8) (2008) 491–495.
[7] A. King, G. Johnson, D. Engelberg, W. Ludwig, Marrow J. Sci. 321 (5887) (2008) 382–385.
[8] C. Soldano, A. Mahmood, E. Dujardin, Carbon 48 (8) (2010) 2127–2150.
[9] J.R. Potts, O. Shankar, S. Murali, L. Du, R.S. Ruoff, Compos. Sci. Technol. 74 (2013) 166–172.
[10] J.R. Potts, O. Shankar, L. Du, R.S. Ruoff, Macromolecules 45 (15) (2012) 6045–6055.
[11] S. Stankovich, R.D. Piner, X. Chen, N. Wu, S.T. Nguyen, R.S. Ruoff, J. Mater. Chem. 16 (2) (2006) 155–158.
[12] H. Kang, K. Zuo, Z. Wang, L. Zhang, L. Liu, B. Guo, Compos. Sci. Technol. 92 (2014) 1–8.
[13] G. Yang, Z. Liao, Z. Yang, Z. Tang, B. Guo, J. Appl. Polym. Sci. 132 (15) (2015) n/a-n/a.
[14] B. Dong, L. Zhang, Y. Wu, Polym. Test. 63 (2017) 281–288.
[15] A. Das, G.R. Kasaliwal, R. Jurk, R. Boldt, D. Fischer, K.W. Stöckelhuber, G. Heinrich, Compos. Sci. Technol. 72 (16) (2012) 1961–1967.
[16] J. Huang, Z. Tang, Z. Yang, B. Guo, Macromol. Rapid Commun. 37 (13) (2016) 1040–1045.
[17] T. Ramanathan, A.A. Abdala, S. Stankovich, D.A. Dikin, M. Herrera-Alonso, R.D. Piner, D.H. Adamson, H.C. Schniepp, X. Chen, R.S. Ruoff, S.T. Nguyen, I.A. Aksay, R.K. Prud'Homme, L.C. Brinson, Nat. Nanotechnol. 3 (6) (2008) 327–331.
[18] Y. Guo, J. Liu, Y. Wu, L. Zhang, Z. Wang, Y. Li, Phys. Chem. Chem. Phys. 19 (33) (2017) 22417–22433.
[19] Z. Tang, X. Wu, B. Guo, L. Zhang, D. Jia, J. Mater. Chem. 22 (15) (2012) 7492.
[20] X. Liu, W. Kuang, B. Guo, Polymer 56 (2015) 553–562.
[21] Z. Yang, J. Liu, R. Liao, G. Yang, X. Wu, Z. Tang, B. Guo, L. Zhang, Y. Ma, Q. Nie, F. Wang, Compos. Sci. Technol. 132 (2016) 68–75.
[22] S. Stankovich, R.D. Piner, S.T. Nguyen, R.S. Ruoff, Carbon 44 (15) (2006) 3342–3347.
[23] J. Wu, G. Huang, H. Li, S. Wu, Y. Liu, J. Zheng, Polymer 54 (7) (2013) 1930–1937.
[24] H. Kim, Y. Miura, C.W. Macosko, Chem. Mater. 22 (11) (2010) 3441–3450.
[25] J.S. Kim, J.H. Yun, I. Kim, S.E. Shim, J. Ind. Eng. Chem. 17 (2) (2011) 325–330.
[26] J.S. Kim, S. Hong, D.W. Park, S.E. Shim, Macromol. Res. 18 (6) (2010) 558–565.
[27] D. Li, M.B. Muller, S. Gilje, R.B. Kaner, G.G. Wallace, Nat. Nanotechnol. 3 (2) (2008) 101–105.

[28] E. Tkalya, M. Ghislandi, A. Alekseev, C. Koning, J. Loos, J. Mater. Chem. 20 (15) (2010) 3035.
[29] J. Yu, K. Lu, E. Sourty, N. Grossiord, C.E. Koning, J. Loos, Carbon 45 (15) (2007) 2897–2903.
[30] D.W. Schaefer, R.S. Justice, Macromolecules 40 (24) (2007) 8501–8517.
[31] Y. Zhan, J. Wu, H. Xia, N. Yan, G. Fei, G. Yuan, Macromol. Mater. Eng. 296 (7) (2011) 590–602.
[32] CN201110057404.0.
[33] CN201510601547.1.
[34] M. Tang, W. Xing, J. Wu, G. Huang, K. Xiang, L. Guo, G. Li, J. Mater. Chem. 3 (11) (2015) 5942–5948.
[35] H. Li, S. Wu, J. Wu, G. Huang, Colloid Polym. Sci. 291 (10) (2013) 2279–2287.
[36] J. Mark, B. Erman, Science and Technology of Rubber, Academic Press, 2005.
[37] M.A. Lopez-Manchado, J. Biagiotti, L. Valentini, J.M. Kenny, J. Appl. Polym. Sci. 92 (5) (2004) 3394–3400.
[38] G. Sui, W. Zhong, X. Yang, S. Zhao, Macromol. Mater. Eng. 292 (9) (2007) 1020–1026.
[39] S. Lakshminarayanan, G.A. Gelves, U. Sundararaj, J. Appl. Polym. Sci. (2012) 5056–5063.
[40] A. Sepehri, M. Razzaghi-Kashani, M.H.R. Ghoreishy, J. Appl. Polym. Sci. 1251 (SI) (2012) E204–E213.
[41] M.A. Lopez-Manchado, M. Arroyo, B. Herrero, J. Biagiotti, J. Appl. Polym. Sci. 89 (1) (2003) 1–15.
[42] A. De Falco, A.J. Marzocca, M.A. Corcuera, A. Eceiza, I. Mondragon, G.H. Rubiolo, S. Goyanes, J. Appl. Polym. Sci. 113 (5) (2009) 2851–2857.
[43] A. Shanmugharaj, J. Bae, K. Lee, W. Noh, S. Lee, S. Ryu, Compos. Sci. Technol. 67 (9) (2007) 1813–1822.
[44] M. Hernández, M.D.M. Bernal, R. Verdejo, T.A. Ezquerra, M.A. López-Manchado, Compos. Sci. Technol. 73 (2012) 40–46.
[45] J. Wu, W. Xing, G. Huang, H. Li, M. Tang, S. Wu, Y. Liu, Polymer 54 (13) (2013) 3314–3323.
[46] W. Xing, H. Li, G. Huang, L. Cai, J. Wu, Compos. Sci. Technol. 144 (2017) 223–229.
[47] A.B. Bourlinos, D. Gournis, D. Petridis, T. Szabó, A. Szeri, I. Dékány, Langmuir 19 (15) (2003) 6050–6055.
[48] H.J. Salavagione, M.A. Gómez, G. Martínez, Macromolecules 42 (17) (2009) 6331–6334.
[49] Z. Xie, X. Fu, L. Wei, M. Luo, Y. Liu, F. Ling, C. Huang, G. Huang, J. Wu, Polymer 118 (2017) 30–39.
[50] Z. Wang, J. Liu, S. Wu, W. Wang, L. Zhang, Phys. Chem. Chem. Phys. 12 (12) (2010) 3014.
[51] G. Heinrich, M. Kluppel, Adv. Polym. Sci. 160 (2002) 1–44.
[52] G. Heinrich, M. Kluppel, T.A. Vilgis, Curr. Opin. Solid State Mater. Sci. 6 (2002). PII S1359-0286(02)00030-X3):195-203.
[53] C. Zhang, S. Huang, W.W. Tjiu, W. Fan, T. Liu, J. Mater. Chem. 22 (6) (2012) 2427–2434.
[54] R. Wang, J. Sun, L. Gao, C. Xu, J. Zhang, Chem. Commun. 47 (30) (2011) 8650.
[55] Z. Tang, H. Kang, Q. Wei, B. Guo, L. Zhang, D. Jia, Carbon 64 (2013) 487–498.
[56] S. Chatterjee, F. Nafezarefi, N.H. Tai, L. Schlagenhauf, F.A. Nüesch, B.T.T. Chu, Carbon 50 (15) (2012) 5380–5386.
[57] S. Yang, W. Lin, Y. Huang, H. Tien, J. Wang, C.M. Ma, S. Li, Y. Wang, Carbon 49 (3) (2011) 793–803.
[58] Y. Li, T. Yang, T. Yu, L. Zheng, K. Liao, J. Mater. Chem. 21 (29) (2011) 10844.
[59] M.K. Shin, B. Lee, S.H. Kim, J.A. Lee, G.M. Spinks, S. Gambhir, G.G. Wallace, M.E. Kozlov, R.H. Baughman, S.J. Kim, Nat. Commun. 3 (1) (2012).
[60] H. Li, L. Yang, G. Weng, W. Xing, J. Wu, G. Huang, J. Mater. Chem. 3 (44) (2015) 22385–22392.
[61] J.R. Shelton, Rubber Chem. Technol. 30 (5) (1957) 1251–1290.
[62] S.B. Munteanu, M. Brebu, C. Vasile, Polym. Degrad. Stabil. 89 (3) (2005) 501–512.
[63] R.M. Lucente-Schultz, V.C. Moore, A.D. Leonard, B.K. Price, D.V. Kosynkin, M. Lu, R. Partha, J.L. Conyers, J.M. Tour, J. Am. Chem. Soc. 131 (11) (2009) 3934–3941.
[64] E.B. Zeinalov, G. Koßmehl, Polym. Degrad. Stabil. 71 (2) (2001) 197–202.
[65] P.C.P. Watts, P.K. Fearon, W.K. Hsu, N.C. Billingham, H.W. Kroto, D.R.M. Walton, J. Mater. Chem. 13 (3) (2003) 491–495.
[66] S. He, Y. Wang, M. Xi, J. Lin, Y. Xue, L. Zhang, Polym. Degrad. Stabil. 98 (9) (2013) 1773–1779.
[67] N. Bitinis, M. Hernandez, R. Verdejo, J.M. Kenny, M.A. Lopez-Manchado, Adv. Mater. 23 (44) (2011) 5229–5236.
[68] Y. Qiu, Z. Wang, A.C.E. Owens, I. Kulaots, Y. Chen, A.B. Kane, R.H. Hurt, Nanoscale 6 (20) (2014) 11744–11755.
[69] F.T. Wang, L. Chen, C.J. Tian, Y. Meng, Z.G. Wang, R.Q. Zhang, M.X. Jin, P. Zhang, D.J. Ding, J. Comput. Chem. 32 (15) (2011) 3264–3268.
[70] J. Yang, Y. Huang, Y. Lv, P. Zhao, Q. Yang, G. Li, J. Mater. Chem. 1 (37) (2013) 11184.
[71] B. Wicklein, A. Kocjan, G. Salazar-Alvarez, F. Carosio, G. Camino, M. Antonietti, L. Bergström, Nat. Nanotechnol. 10 (3) (2015) 277–283.
[72] J. Wu, L. Zeng, X. Huang, L. Zhao, G. Huang, J. Mater. Chem. 5 (29) (2017) 15048–15055.
[73] W. Xing, J. Wu, G. Huang, H. Li, M. Tang, X. Fu, Polym. Int. 63 (9) (2014) 1674–1681.
[74] W. Xing, M. Tang, J. Wu, G. Huang, H. Li, Z. Lei, X. Fu, H. Li, Compos. Sci. Technol. 99 (2014) 67–74.